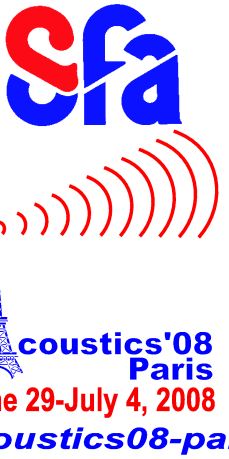

euronoise

Audio acoustic modeling using full-wave methods

Timo Lahivaara, Tomi Huttunen and Simo-Pekka Simonaho

University of Kuopio, P.O.Box 1627, 70211 Kuopio, Finland
simo-pekka.simonaho@uku.fi

The numerical simulation of wave propagation poses a significant challenge in scientific computation. Historically, several approaches are explored in order to get a stable method that can be efficiently used for approximating wave propagation without excessive numerical dissipation or dispersion. Unfortunately, the traditional approaches, such as the finite element and the finite difference, require many discretization points per wavelength to obtain reliable solutions. In this study, two alternative full-wave methods for reducing the computational complexity are consider. The methods are the time-domain discontinuous Galerkin method and the ultra weak variational formulation in the frequency domain. Using these techniques, the directivity patterns and the frequency response of a loudspeaker are studied. Moreover, the simulated results are compared to experimental measurements.

1 Introduction

The modeling of the acoustic wave fields often provides additional information for acoustical measurements. In the case of long wavelengths, wave problems can be modeled using full-wave type methods which include the finite element, finite difference and boundary element methods. Unfortunately, when the wavelength decreases, these traditional full-wave modeling techniques become increasingly expensive since a sufficient number of discretization points per wavelength (10 points per wavelength is considered as the rule of thumb) is required to obtain a reliable solution. In addition, the numerical pollution due to the accumulation of phase error forces the use of even more grid points per wavelength to keep the relative error of solutions sufficiently low.

Promising candidates for solving the wave propagation problems with a reduced computational cost are the ultra weak variational formulation (UWVF [3] (Waveller software [6] used in this study)) (in the frequency domain) and the discontinuous Galerkin (DG) [5] (in the time-domain). These approaches use same computation meshes as the standard finite element method. However, the idea of the UWVF approach is that the sound field can be computed elementwise using plane wave basis functions. In most cases, the use of the plane wave basis significantly reduces the need of CPU-time and memory compared to conventional techniques (such as the finite element method).

In the time-domain DG method the high-order Legendre polynomial basis are used. In general, the Legendre basis is a common choice for the DG method.

In this study, the UWVF and DG methods are used for approximating the wave propagation in three spatial dimensions (3D). We consider geometry which contains a real loudspeaker in free space. Results are computed using the MPI parallelized FORTRAN90 UWVF code (Waveller) and MPI parallelized C++ DG solver codes. The used PC-cluster contains 24 Pentium 4 with 96 GB total RAM. The main goal of this work is to study the directivity pattern and frequency response of the loudspeaker. In addition, these results are compared to experimental measurements.

2 Numerical Methods and Measurement System

In this section, the numerical methods for the wave equation are summarized and the measurement system is outlined. In this study, the full-wave solution means the numerical solution of the acoustical wave equation. The wave equation is approximated in the frequency domain using the UWVF method and in the time-domain using the DG method.

As the mathematical model we assume that Ω is a bounded Lipschitz domain in $\mathbb{R}^3$, Γ is its boundary, $\boldsymbol{x} = (x, y, z) \in \Omega$ is the spatial variable and $t \in [0, T]$ time. Then, the linear acoustic wave equation with the boundary condition on the boundary Γ and initial condition with $t = t_0$ can be written as

$$\frac{1}{c^2\rho}\frac{\partial^2 u}{\partial t^2} = \nabla \cdot \left(\frac{1}{\rho}\nabla u\right) \quad \text{in } \Omega, \tag{1}$$

$$\frac{\partial u}{\partial t} = u_0 \quad \text{at } t = t_0, \tag{2}$$

$$u = u_1 \quad \text{at } t = t_0, \tag{3}$$

$$\sigma\frac{\partial u}{\partial t} + n \cdot \left(\frac{1}{\rho}\nabla u\right) = Q\left(-\sigma\frac{\partial u}{\partial t} + n \cdot \left(\frac{1}{\rho}\nabla u\right)\right) + \sqrt{2\sigma}g \quad \text{on } \Gamma, \tag{4}$$

where u is the acoustic pressure, c is the wave speed and ρ is the density. In Eqs. (2) and (3) the u_0 and u_1 contain the given initial values and in Eq. (4) n is the outward unit normal of the boundary Γ, g is a source function, and σ is a real and positive parameter. The Helmholtz problem is obtained by assuming that the acoustic pressure field is time-harmonic, i.e. $u(\boldsymbol{x}, t) = \hat{u}(\boldsymbol{x})e^{-i\omega t}$. The truncation of an unbounded problem is done using the perfectly matched layer (PML) [1], which is a numerical damping layer surrounding the computational domain.

For the DG and UWVF methods, the domain Ω is partitioned into a collection of finite elements (tetrahedra are a natural choice in 3D). After the partitioning, the weak formulation can be written individually for each element. Furthermore, the communication between adjacent elements is handled using a numerical flux. The final weak form for the problem is obtained by summing over all of the elements. The more detailed derivation for the UWVF method can be found from [2] and for the DG method from [4]. In this paper the time integration of the DG method is carried out using the Crank-Nicolson time integration method.

The DG and UWVF methods are used for simulating the directivity of a loudspeaker. The simulations are compared with experimental measurements. The directivity pattern of a loudspeaker was measured in the semi anechoic chamber. To avoid the floor reflection, the floor between loudspeaker and the microphone was covered with plastic foam wedges (see Fig. 1). In the measurement, the sine wave was fed to the loudspeaker and its

response on the acoustical axis was measured. Next, the loudspeaker was rotated and its response measured again. The measurements were performed using B&K 4954 free-field microphone. The distance between the microphone and loudspeaker was 1 m. The amplitude of the sine wave was set to be 94 dB on the acoustical axis of the loudspeaker. The measurements were performed in 5 degrees interval in the angle from -30 to 30 and -60 to 60 degrees around the acoustic axis in yz-plane and xz-plane, respectively.

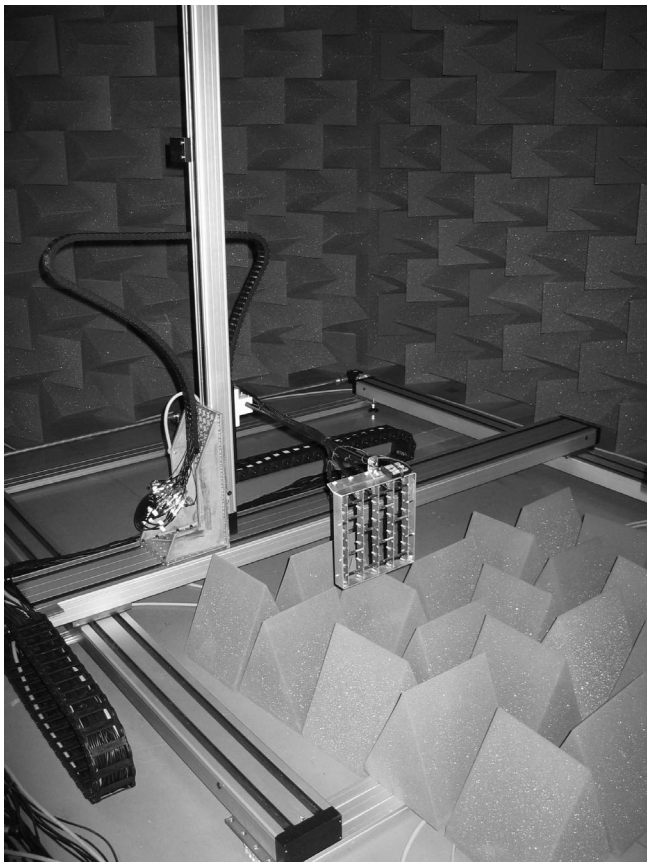

Fig. 1: The measurement system with the microphone array consists of 6 × 5 microphones (Panasonic WM-61A capsules).

Measurements were also performed using microphone array and an automated scanning system. The microphone array consists of 6 × 5 microphones (Panasonic WM-61A capsules). The distance between adjacent microphones was 5 cm (see Fig. 1). The microphone array is initially positioned at a corner of the measurement area. Next, the stimulus signal is fed to loudspeaker and the response is measured. All 30 channels were recorded simultaneously using 24-bit data acquistion hardware. After data acquistion, the microphone array is moved to the next measurement position and data is acquired again. This process is repeated until the whole measurement area is covered. Synchronization between the loudspeaker and the data acquistion is controlled with the data acquistion hardware. The stimulus signal triggers the response measurements and in this way one can assume that all data is acquired simultaneously. The stimulus signal was generated using Eq. (7). The measurement area was 100 × 100 cm^2 and distance between adjacent measurement points was 2.5 cm.

3 Numerical Experiments

In this section numerical examples are studied. Let us consider the wave propagation in homogeneous medium. In particular, our focus in the following simulations is to study the directivity and the frequency response of the loudspeaker. In all of the simulations the wave propagation is studied in air. More precisely the speed of sound c and the density ρ are 340 m/s and 1.2 kg/m^3, respectively. Attenuation is ignored in all cases.

Before calculations we need to generate the problem geometry. The problem geometry consists of the loudspeaker and the surrounding free space. First, we generate the loudspeaker geometry from its CAD geometry file using the Gambit® software. Then, the Comsol Multiphysics software® was used to make the free space geometry (box with the PML region). After that, we unite the loudspeaker geometry in the box. Before the simulations, the problem geometry needs to be partitioned into elements i.e. into the computational mesh. For that purpose the Comsol Multiphysics® software was used.

Fig. 2 shows the problem geometry. In Fig. 2 the volume between the inner and the outer cube is the PML region. The thickness of the PML is 69 cm in all simulations. The dimension of the computational domain is $\Omega = [-1.725,\ 1.725]^3$ m.

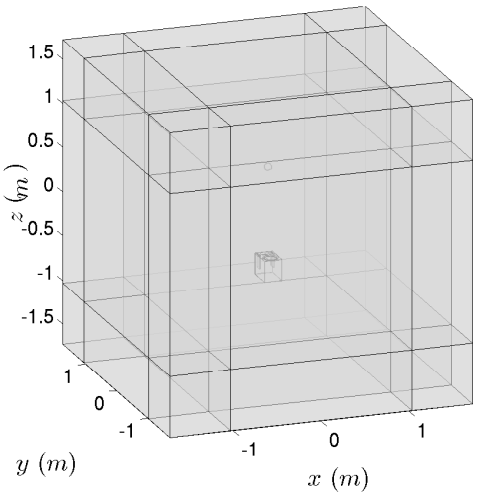

Fig. 2: The problem geometry which contains the sound source (loudspeaker located in free space). Figure shows also the PML region(s).

The source is introduced to the model by using an inhomogeneous Neumann boundary condition on the bass surface. Other parts of the loudspeaker are handled using the sound-hard boundary condition, except the end of the reflex tube, which contains the absorbing boundary condition. Finally, the exterior boundaries of the problem geometry have the absorbing boundary condition.

Before going any further, two stability indicators for the solutions must be introduced. In this study we want to control the grid density and the Courant-Friedrichs-Lewy (CFL) number. The indicator of the grid density shows how many approximation points there are

per wavelength. This can be presented as

$$N = \frac{\lambda}{h_{\max}}, \tag{5}$$

where λ is the wavelength, $h_{\max}$ is the longest distance between two nodes of a single element in the computation mesh and N is the number of points per wavelength. For the time-domain solutions also the CFL number must be controlled. The CFL number can be written as follows

$$\mathrm{CFL} = \frac{c\delta_t}{h_{\min}}, \tag{6}$$

where c is the speed of sound, δ_t is the length of the time step and $h_{\min}$ is the smallest distance between two nodes of the the computational mesh. In all simulations the CFL number is equal to 0.02.

The computation mesh is shown in Fig. 3. In Fig. 3 the cross-section of the whole mesh and also the surface mesh of the loudspeaker are shown. One must note that the source surface is shown in different color in the surface mesh. Computation meshes consists of 463692 ($h_{\max}$ = 194.7 mm and $h_{\min}$ = 78.3 mm) elements. For the directivity pattern simulations sine wave at frequency of 1000 Hz is used, from which we obtain the grid density $N \approx 1.7463$ (5). Respectively, for the frequency response simulations the frequency of 2000 Hz is used (the mean frequency of the gaussian pulse), which gives $N \approx 0.8732$ (5).

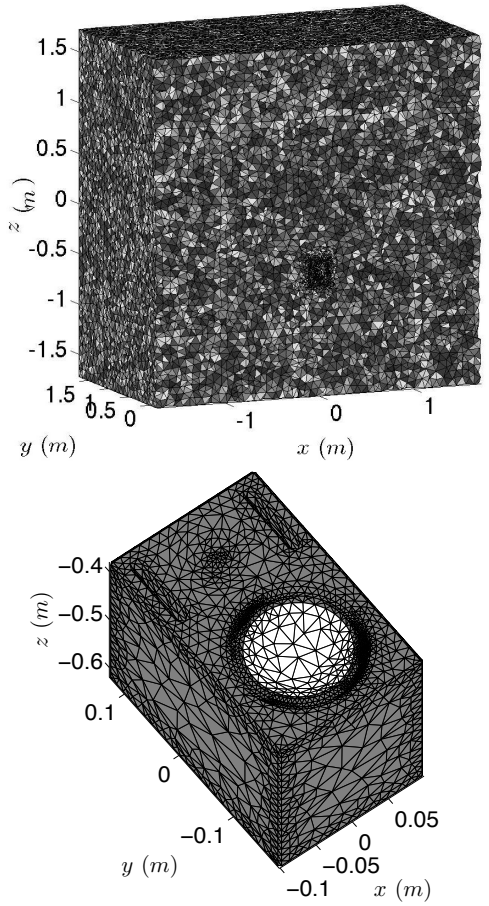

Fig. 3: Mesh used in the computations. Top: The mesh consists of 463692 elements. Bottom: The surface mesh of the loudspeaker. One must note that in the surface mesh the sound source is shown with different color.

The directivity patterns are shown in Fig. 4. It can be seen from Fig. 4(a) that the pattern is symmetric in the xz-plane. In the yz-plane it is interesting to notice how the asymmetry of the speaker affect on the shape of the solution. The diffraction of the field behind the loudspeaker (xz and yz planes) can also be seen from the directivity patterns.

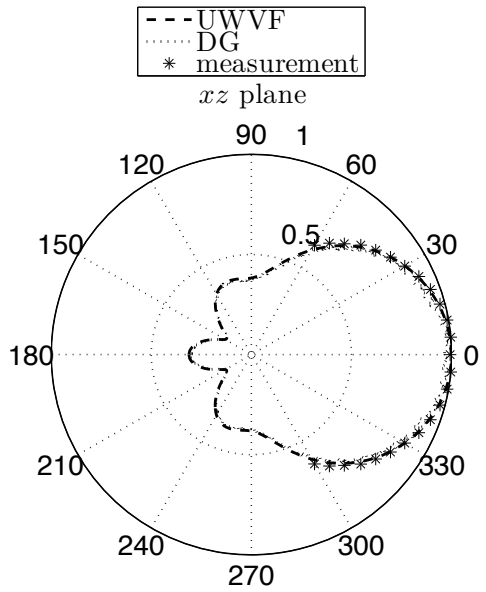

(a)

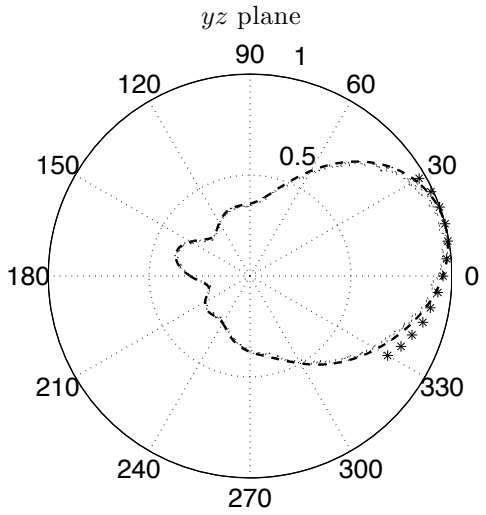

(b)

Fig. 4: The directivity patterns at 1000 Hz. The title shows the studied plane. Both figures contains the numerical solutions and the measurement. The measurements are carried out with angle [-60:5:60]° in the xz-plane and [-30:5:30]° in the yz-plane.

Fig. 5 shows the frequency response of the loudspeaker. Results are shown in the frequency domain (normalized pressure field as a function of frequency) and in the time-domain (normalized pressure field as a function of time). The conversion between the time and frequency domain is carried out using the Fourier transform. These results are computed at the acoustics axis at the distance of 1 m. The sound source for the time-domain simulations is written as follows

$$g = \exp\left(-\left(x_b\left(t - t_0\right)\right)^2\right)\sin\left(\omega\left(t - t_0\right)\right), \tag{7}$$

where $x_b = 2000$, t is the time, $t_0 = 0.001$ and ω denotes the angular frequency.

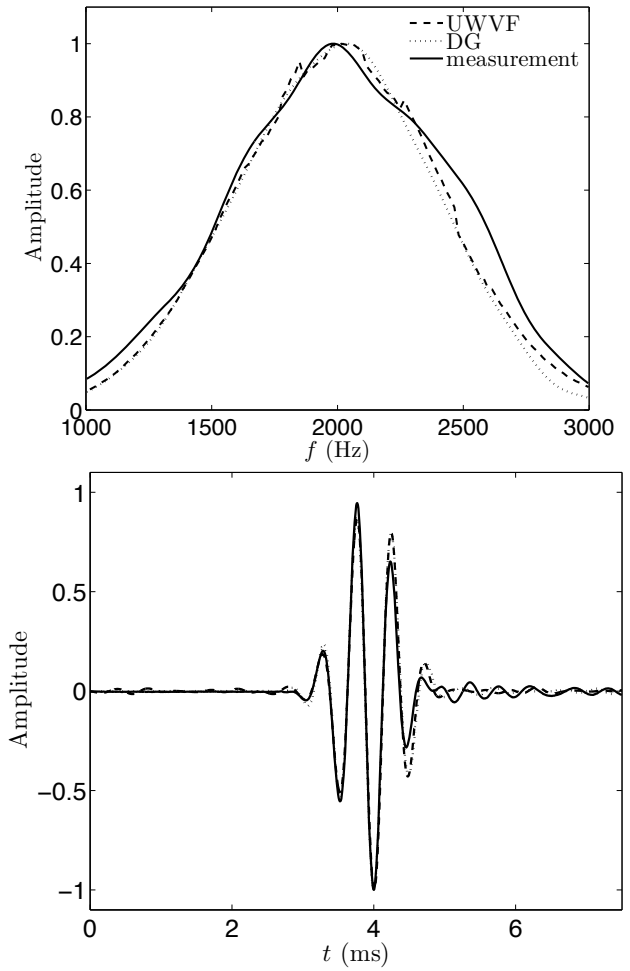

Fig. 5: The frequency response at the acoustic axis (1 m). A normalized pressure amplitude as a function of the frequency (Top) and time (Bottom). Both figures shows two numerical solutions (DG and UWVF) and measurement. Measurements is performed using a B&K 4954 microphone.

Finally, Figs. 6 and 7 show the pressure fields. Fig. 6 shows the sound pressure level in decibels and real-part of the pressure field at a single frequency (1000 Hz) which are computed using the UWVF method.

In Fig. 7 the pressure fields are shown in a plane at a single time instant of the DG simulation and experimental measurement. These results are shown in normalized pressure amplitude scale.

4 Conclusions

In this work the wave equation equation is solved in 3D using the UWVF method in frequency domain and the DG method in the time-domain. The main goal of the work was to study the directivity and frequency response of the loudspeaker. The geometry of the problem contained the real geometry of the loudspeaker in free space. Numerical solutions were computed using the parallelized UWVF (Waveller software) and DG solvers and these results were compared to measurements.

As a conclusion it can be seen from Fig. 4 where the directivity patterns of the loudspeaker were simulated

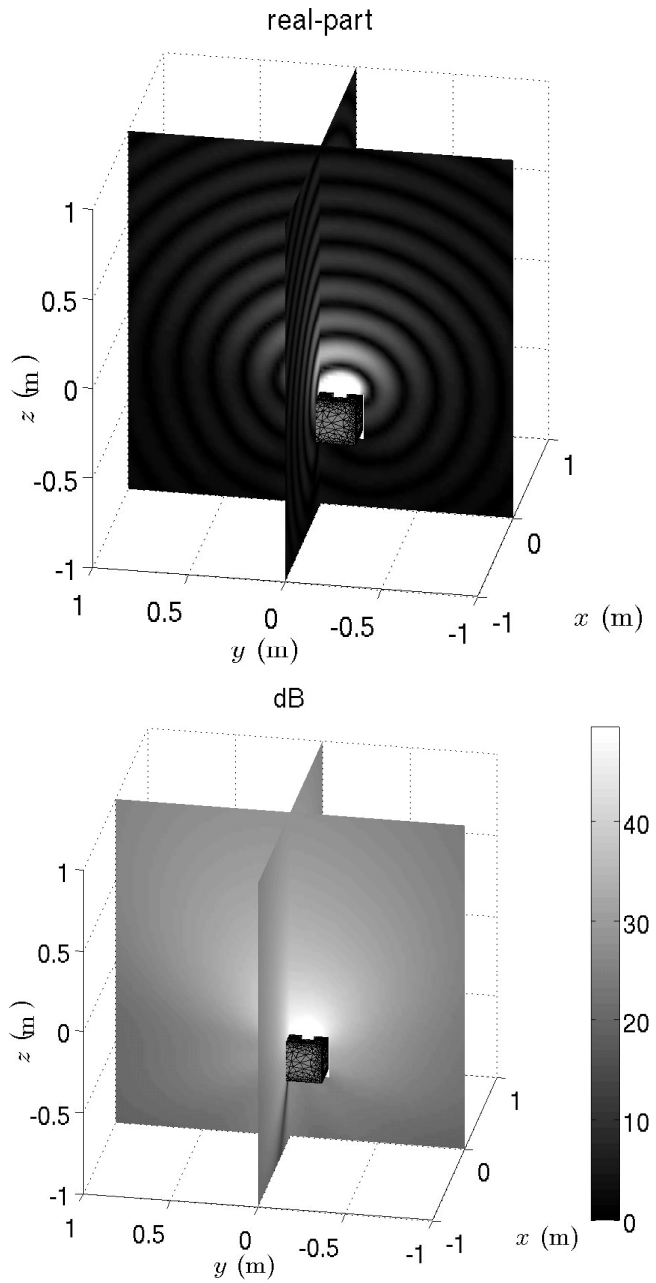

Fig. 6: An example solution computed using the UWVF method at 1000 Hz. Top: The real-part of the pressure field. Bottom: The sound pressure level in decibels (colorbar shows the dB value).

that a good accuracy can be obtained using the both methods. On the other hand, Fig. 5 shows that the frequency response of the used sound source can be also approximated with satisfactory accuracy. Finally, Fig. 7 shows that the modeled pressure field in the single plane agrees well with the corresponding measurement. Nevertheless, while the results show that simulation of the loudspeaker is possible, a detailed comparison with measurements still needs to be made to validate the simulation accuracy.

The simulation model can be further improved. For example, one must note that our model does not approximate the reflex tubes correctly. This is handled only by using the absorbing boundary condition at the end of the tube. The model for loudspeaker surface would also be better by using the real surface impedance of the

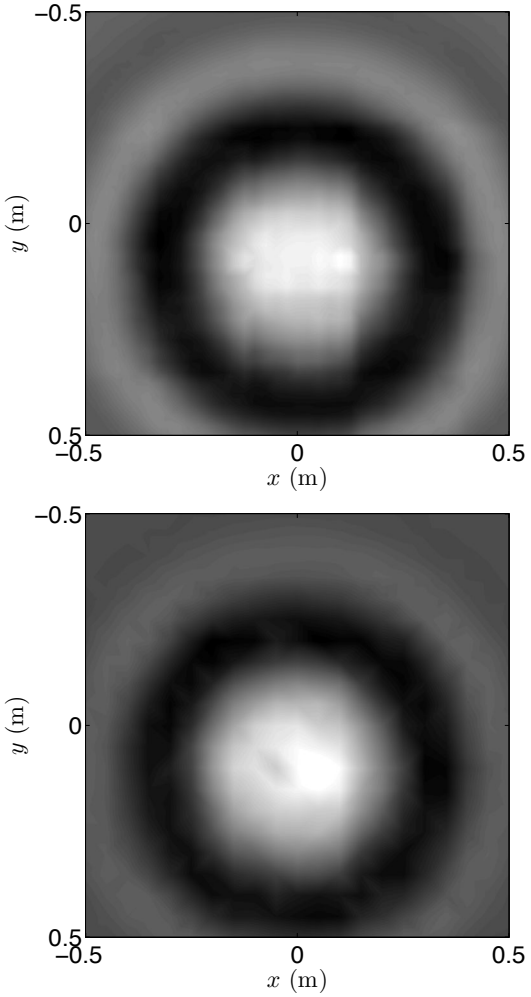

Fig. 7: Pressure fields in the time-domain (normalized pressure amplitude) at the time instant 1.9 ms (on the acoustic axis at 60 cm distance from the loudspeaker). Top: Numerical solution using the DG method. Bottom: Measured pressure field.

loudspeaker material.

Acknowledgments

The authors wish to thank the Finnish Funding Agency for Technology and Innovation (Tekes) and the European Regional Development Fund (ERDF) for financial support. This work was also supported by the Academy of Finland (application number 213476, Finnish Programme for Centres of Excellence in Research 2006-2011) and by the Finnish IT center for science (CSC).

References

[1] J. Bérenger, "A perfectly matched layer for the absorption of electromagnetic waves", *J. Comput. Phys.*, 185-200 (1994)

[2] T. Huttunen, "The Ultra Weak Variational Formulation for Ultrasound Transmission Problems", *PhD thesis, University of Kuopio*, (2004)

[3] B. Després, "Sur une formulation variationnelle de type ultra-faible", *Comptes Rendus de l'Academie des Sciences - Series I*, 939-944 (1994)

[4] P. Monk, R. Richter, "A discontinuous Galerkin method for linear symmetric hyperbolic systems in inhomogeneous media", *J. Sci. Comp.*, 443-477 (2005)

[5] W. Reed, T. Hill, "Triangular mesh methods for the neutron transport equation", *LA-UR-73-479, Los Alamos National Laboratory, Los Alamos, New Mexico, USA*, (1973)

[6] "www.waveller.com"